

# LOCALIZATION OF SECTIONS WITHIN THE BRAIN VIA 2D TO 3D IMAGE REGISTRATION

*Smadar Gefen<sup>1</sup>, Louise Bertrand<sup>1</sup>, Nahum Kiryati<sup>2</sup>, and Jonathan Nissanov<sup>1</sup>*

<sup>1</sup>Laboratory for Bioimaging and Anatomical Informatics, Department of Neurobiology & Anatomy,  
Drexel University College of Medicine  
2900 Queen Lane, Philadelphia, PA 19129

<sup>2</sup>School of Electrical Engineering, Tel-Aviv University  
Tel-Aviv 69978, Israel

## ABSTRACT

Mouse Brain Library (MBL) is a database of brain images, each consisting of sparse coronal or horizontal sections. To facilitate morphometric research, it is necessary to index each of these sections by its location within a canonical 3D atlas (NeuroTerrain). This is done with a 2D to 3D matching technique which was developed in this study. The registration method is image-based and uses a genetic algorithm to find the local-affine transformation that maximizes a mutual information metric. The average distance between the registration results achieved with the proposed method as compared with manual matching by an expert was 250 microns. This compares well with repeated manual trials where inter-trial matching distance was on average 200 microns.

## 1. INTRODUCTION

The MBL is a neuroinformatic resource aimed at assisting neurogeneticists [1]. The library contains a large collection of brain images from inbred strains of mice that can be used in a type of genetic mapping approach called quantitative trait analysis. The essence of this approach is to compare morphometric and genetic variations between strains. A key neuroinformatic solution required in this setting is an effective brain normalization algorithm to support automated morphometric analysis. Our approach is to register MBL sections to a reference 3D atlas by first matching sections to the corresponding atlas plane, and then by a 2D warping [2]. Here we focus on the first matching step of the approach.

There are several previously reported methods for 2D to 3D brain mapping. Kim et al. [3], for instance, performed motion correction by mapping each slice of functional magnetic resonance imaging image (fMRI) onto the volumetric MR image which was acquired in the same session by using a rigid-body transformation. Simulation of this registration method yielded average translational error of 0.043mm and rotational error of 0.065°. Registration of postmortem brain slices to MRI volume was proposed by Kim et al. [4], with non-linear polynomial transformations. Simulation experiments yielded correlation of 0.9952 [4]. In this study histological brain images of an experimental dataset and of an atlas were first globally aligned

based on their external surfaces. Then, further alignment was achieved by locally registering each section from the experimental dataset to the atlas volume.

The registration of a brain section to a 3D atlas is a global optimization problem. To illustrate this, we initiated a local steepest descent search from each of 100 randomly selected points in the search space. This yielded many different solutions, thus proving the necessity for a global optimization algorithm. It is well known that, in the worst case, the global maximum of a function within a continuous search space cannot be found in finite time [5]. Nevertheless, many global optimization algorithms have been developed which are problem dependent [6]. Genetic Algorithms [7, 8] have also been successfully applied to a large variety of global optimization problems. Genetic Algorithms are used in this research.

## 2. ALGORITHM DESCRIPTION

The localization of sections from the experimental dataset within an atlas volume involves a 2D to 3D registration operation in which a coronal section  $I_e$  is matched with the corresponding 2D plane within the atlas volume  $I_a$ . Figure 1 shows the atlas coordinate system with the brain centered within a 608 by 320 by 1104 voxel box, where a voxel is 17.9 micron isotropic. Here, a 2D plane in the atlas space is defined by its crossing point with the  $z$  axis and its rotation angles  $\alpha_x$  and  $\alpha_y$  with respect to the  $x$  and  $y$  axes, respectively.

The registration of a section,  $I_e$ , onto its corresponding plane,  $I_a$ , was done in two steps. First, the affine transformation that matches the reconstructed experimental brain dataset surface with the atlas surface was found. This was done using a 3D surface-based registration algorithm described in [9]. We refer to this part of the algorithm as *global-affine* registration. Thus, using the *global-affine* transformation any coronal section from the experimental dataset could be aligned with the atlas yielding  $I_e^{ga}$ . Next,  $I_e^{ga}$  was locally registered to its corresponding plane within the atlas, yielding  $I_e^{la}$ . This image-based affine registration, referred to here as *local-affine* registration, does not compensate completely for the

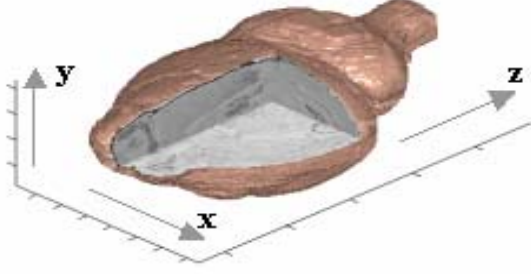


Fig. 1. The atlas coordinate system with the brain centered within a 608 by 320 by 1104 voxel box, where a voxel is 17.9 micron isotropic

discrepancies between  $I_e$  and  $I_a$ , but rather brings them closer before further nonlinear matching is employed.

In order to locally match an experimental section with its corresponding plane within the atlas the following mapping parameters need to be defined:

$$\boldsymbol{\theta} \equiv [\alpha_x, \alpha_y, z, R_{11}, R_{12}, R_{21}, R_{22}, d_1, d_2]. \quad (1)$$

$\boldsymbol{\alpha} = [\alpha_x, \alpha_y]$  and  $z$  define a plane within the atlas volume and the matrix  $\mathbf{R} = [R_{11}, R_{12}, R_{21}, R_{22}]$  and the displacement vector  $\mathbf{d} = [d_1, d_2]$  define the affine mapping that is applied to the given experimental section,  $I_e^{ga}$ .

Although both the experimental dataset and the atlas are histological images, due to differences in preparation of the brain tissues and due to image acquisition protocols, the intensity and texture of corresponding regions are not similar (see differences in brightness between figure 3(a) and 3(b-d)). Therefore, a Mutual Information (MI) metric was chosen to measure the alignment degree in the optimization process [10]:

$$MI(I_e^{la}, I_a) = \sum_i \sum_j p(i, j) \log \frac{p(i, j)}{p(i)p(j)}, \quad (2)$$

where  $i$  and  $j$  denote random variables that take the intensity values of corresponding pixels from  $I_e^{la}$  and  $I_a$ , respectively. A normalized joint intensity histogram was used to estimate the joint and marginal probabilities.

A genetic algorithm was used to search for the parameter vector  $\boldsymbol{\theta}$  that yields the best match between the given experimental section and its corresponding plane within the atlas. There are three main operations that take place when employing a genetic optimization method: selection, mutation, and crossover. The selection operation selects with replacement the best solution pairs ("parents") that exist within the current pool of solutions ("generation"). These selected solution pairs will be used later to generate the new generation of solutions. Next, the two other operations, mutation and crossover, are applied. Mutation is the operation that increases variation within the pool of solutions, producing new random solutions within

the given range to be explored. Crossover is the operation that merges two good solutions, and, in doing so, results in convergence.

The optimization algorithm first generates a population of  $J$  solutions,  $\{\boldsymbol{\theta}_{k=0}^j; j = 1 : J\}$ , within a range of  $[\boldsymbol{\theta}_{\min}, \boldsymbol{\theta}_{\max}]$ , as follows:

$$\boldsymbol{\theta}_{k=0}^j[n] = \begin{cases} \boldsymbol{\theta}_0[n] + (\boldsymbol{\theta}_{\max}[n] - \boldsymbol{\theta}_0[n]) \cdot r & p \leq 0.5 \\ \boldsymbol{\theta}_0[n] - (\boldsymbol{\theta}_0[n] - \boldsymbol{\theta}_{\min}[n]) \cdot r & p > 0.5 \end{cases} \quad (3)$$

where  $n$  is an index for the elements in the vector  $\boldsymbol{\theta}$ ,  $\boldsymbol{\theta}_0$  is an initial parameter vector,  $k$  the iteration index, and  $r$  and  $p$  are random numbers uniformly distributed between 0 and 1.

Next, the following steps are carried out iteratively:

#### 1) Selection:

- $N$  2D planes  $I_a$  are extracted from the atlas space, based on the parameters  $\boldsymbol{\alpha}_k = [\alpha_x, \alpha_y]_k$  and  $z_k$  from the current solution pool.
- $N$  experimental sections  $I_e^{la}$  are computed based on the parameters  $\mathbf{R}_k$  and  $\mathbf{d}_k$  from the current solution pool.
- The Mutual information metric,  $MI_k(I_e^{la}, I_a)$ , is computed.
- Each solution,  $\boldsymbol{\theta}_k$ , is assigned a probability that is proportional to its mutual information,  $MI_k(I_e^{la}, I_a)$ .
- A new set of solutions,  $\{\boldsymbol{\theta}_k^j; j = 1 : J\}$ , is selected with replacement based on its assigned probability.

#### 2) Mutation:

The new pool of solutions is then mutated, with a probability that was set to 0.1, as follows:

$$\boldsymbol{\theta}[n]_k^j = \begin{cases} \boldsymbol{\theta}[n]_k^j + (\boldsymbol{\theta}[n]_{\max} - \boldsymbol{\theta}[n]_k^j) \cdot (1 - r^c) & p \leq 0.5 \\ \boldsymbol{\theta}[n]_k^j - (\boldsymbol{\theta}[n]_k^j - \boldsymbol{\theta}[n]_{\min}) \cdot (1 - r^c) & p > 0.5 \end{cases} \quad (4)$$

where  $c = (1 - k / K)^b$ ,  $K$  is the total number of iterations, and  $b$  is a positive number ( $\neq 5$ ).  $c$  controls the maximum amplitude of parameter mutation and decreases as the number of iterations increases.

#### 3) Crossover:

Out of each two consecutive solutions,  $\boldsymbol{\theta}_k^j$  and  $\boldsymbol{\theta}_k^{j+1}$ , in the current pool, a new pair of solutions,  $\boldsymbol{\theta}_{k+1}^j$  and  $\boldsymbol{\theta}_{k+1}^{j+1}$ , is created and included in the next generation of the solution pool:

$$\begin{aligned} & [\theta[n]_{k+1}^j, \theta[n]_{k+1}^{j+1}] = \\ & \begin{cases} (\theta[n]_k^j + \theta[n]_k^{j+1}) / 2, & \theta[n]_k^{j+1} & p < 0.4 \\ (\theta[n]_k^j + \theta[n]_k^{j+1}) / 2, & \theta[n]_k^j & p > 0.6 \\ \theta[n]_k^j, & \theta[n]_k^{j+1} & o/w \end{cases} \quad (5) \end{aligned}$$

#### 4. EXPERIMENTS

The section-to-volume registration algorithm, described above, was demonstrated by registering 20 coronal sections from three mouse brains (genetic strain C57BL/6J) onto a mouse atlas [11]. The experimental brain datasets were generated as follows: mouse brains were embedded in celloidin, was cut coronally into 30 microns sections, stained with cresyl violet, and then imaged with an in-plane resolution of 4.4 microns [12].

The atlas brain was generated employing a slightly different procedure. A mouse brain was dissected and stored at  $-80^\circ\text{C}$ . Next, the brain was embedded in a mixture of Lipshaw M-1 medium and India Ink medium to allow the mounting of the brain within the microtome for accurate sectioning into 17.9 micron sections. Sections were then collected on slides, dried overnight, and stained with cresyl violet. Later, sections were scanned with 8 micron resolution. The reconstruction of these sections' images into a 3D volume was done by, first, aligning the sections to their corresponding block-face images and, second, employing a section-to-section image based registration [13]. Finally, the aligned images were scaled, yielding a three-dimensional 17.9 micron isotropic volume [14].

In order to evaluate the efficacy of the local affine algorithm, we registered a sample of atlas sections onto the atlas volume. In this setting linear (local-affine) transformations should lead to an accurate solution for the registration parameters. Since in this case the true solution for the alignment parameters is known, we can evaluate the rate of convergence of the applied optimization algorithm. The registration error in this case is measured as the average Euclidian distance between the atlas section found by the registration algorithm and the known corresponding atlas section. Table I shows this alignment error and algorithm running time (based on algorithm implementation using MATLAB on a Pentium IV PC with 1.9 GHz and 2 GB RAM) as a function of iteration number. Figure 2 shows the maximum MI value of the solution population as a function of iterations.

Evaluation of registration accuracy when applied to experimental data requires a gold-standard. In this study we used a standard that was computed based on the manual registration of a subset of experimental sections as done by an expert. Note that the accuracy of the local-affine registration is limited by the fact that the spatial deformation that exists between experimental data and the atlas is a non-linear 3D deformation (inter-subject).

The manual registration was performed for a subset of experimental sections 120 microns apart (every fourth section). Each section in this subset was independently aligned twice with substantial time delay between each trial to eliminate possible correlation between trials. The parameters  $\mathbf{a}_m = (\mathbf{a}_1 + \mathbf{a}_2) / 2$  and  $z_m = (z_1 + z_2) / 2$  were found for each section in the subset. Then, the parameters for the rest of the sections were

estimated by interpolation. This is not an easy task for an operator: the average difference between repeated trials was found to be 200 microns.

The accuracy of this registration algorithm was evaluated by examining the average distance between the atlas plane selected by the algorithm as the best match to the experimental section and the atlas plane selected by an expert. Figure 3 shows an experimental section (a) and its manually selected

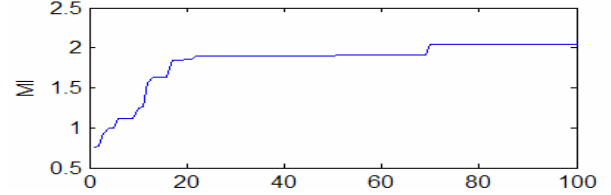


Fig. 2. The solution population maximum MI value as a function of the number of iterations.

corresponding plane from the atlas (b). The global-affine alignment mapping is shown in (c). A further local-affine alignment (employing 50 iterations) is shown in (d). The proximity between the choice of the expert and the algorithm results is apparent.

Tables II and III show the average error when applying the 2D-3D alignment algorithm described above to 20 coronal sections from three experimental brain dataset. Table II shows the average error after applying global-affine alignment and Table III shows the average error after applying the local-affine alignment. It can be seen that there is about a two-fold improvement in alignment.

TABLE I: ATLAS SECTION TO ATLAS VOLUME LOCAL-AFFINE REGISTRATION - AVERAGE ERROR AND SPEED AS A FUNCTION OF ITERATION NUMBER

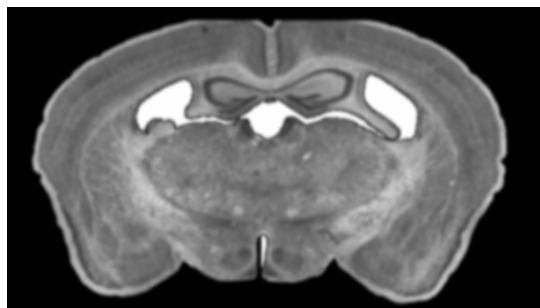
Iter. No.	Mean	Med.	Min	Max	time [Min.]
10	4.21	3.89	0.28	10.47	3.33
20	2.56	2.40	0.12	6.25	6.32
30	1.85	1.76	0.05	4.46	9.27

TABLE II: EXPERIMENTAL SECTION TO ATLAS VOLUME GLOBAL-AFFINE REGISTRATION - AVERAGE ERROR (VOXELS)

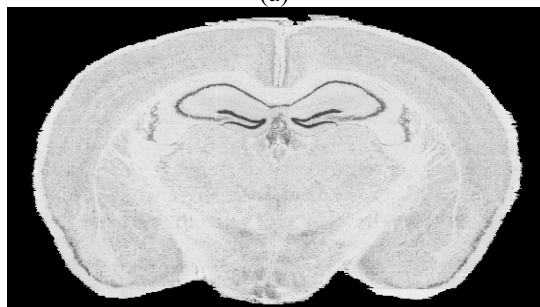
	Mean	Median	Min	Max
Br1556	21.73	20.09	0.34	54.82
Br1557	23.24	21.69	0.00	59.06
Br1558	25.86	24.16	0.00	66.74
<b>Average</b>	<b>23.61</b>	<b>21.98</b>	<b>0.11</b>	<b>60.20</b>

TABLE III: EXPERIMENTAL SECTION TO ATLAS VOLUME LOCAL-AFFINE REGISTRATION - AVERAGE ERROR (VOXELS)

	Mean	Median	Min	Max
Br1556	12.95	11.80	0.33	32.39
Br1557	14.63	13.48	0.22	37.25
Br1558	15.41	14.25	1.11	38.32
<b>Average</b>	<b>14.33</b>	<b>13.18</b>	<b>0.55</b>	<b>35.99</b>



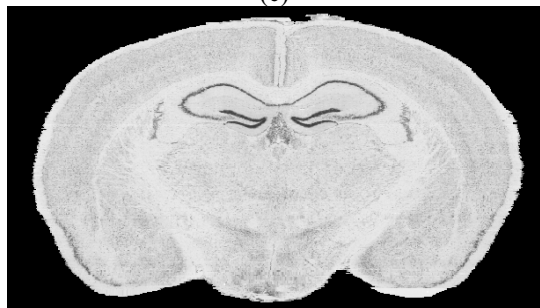
(a)



(b)



(c)



(d)

Fig. 3. An experimental section (a) and its manually selected corresponding plane from the atlas (b). The image in (c) shows the corresponding plane based on global-affine alignment. The image in (d) shows the corresponding plane based on local-affine alignment. The similarity between (d) and (a) is especially noticeable in the hippocampal region.

## 5. SUMMARY

Localization of an experimental brain section within the volume of an atlas is a complex task even for an expert. In part, this is because of the normal anatomical variability between subjects,

and, in part, because a section's true position within the atlas is on a surface and not on a plane. In this study a method that matches a section with a plane within the atlas was proposed. A genetic algorithm was used to find the transformation that maximizes a mutual information metric between a given section and its corresponding atlas plane. The results obtained with this method are consistent with an expert's manual registration performance to within an average distance of 250 microns.

*Acknowledgement:* This work was supported by the Human Brain Project through grant P20 MH62009 funded jointly by NIMH, NIDA, and NSF.

## 11. REFERENCES

- [1] G. D. Rosen, et al., "Informatics Center for Mouse Genomics: The Dissection of Complex Traits of the Nervous System," *Neuroinformatics*, vol. 1, pp. 327-342, 2003.
- [2] S. Gefen, J. O. Tretiak, L. Bertrand, G. D. Rosen, and J. Nissanov, "Surface Alignment of an Elastic Body Using A Multi-resolution Wavelet Representation," *IEEE Transaction on Biomedical Engineering*, vol. 51, pp. 1230-1241, 2004.
- [3] B. Kim, J. L. Boes, P. H. Bland, T. L. Chenevert, and C. R. Meyer, "Motion Correction in fMRI via Registration of Individual Slices Into an Anatomical Volume," *Magnetic Resonance in Medicine*, vol. 41, pp. 964-972, 1999.
- [4] T. S. Kim, M. Singh, W. Sungkarat, C. Zarow, and H. Chui, "Automatic Registration of Postmortem Brain Slices to MRI Reference Volume," *IEEE Tran. on Nuclear Science*, vol. 47, pp. 1607-1613, 2000.
- [5] A. Torn and A. Zilinskas, *Global Optimization*, vol. 350: Springer, 1989.
- [6] D. H. Wolpert and W. G. MacReady, "No Free Lunch Theorems for Optimization," *IEEE Transactions on Evolutionary Computation*, vol. 1, pp. 67-82, 1997.
- [7] D. Whitley, "A Genetic Algorithm Tutorial," Dept. of Computer Science, Colorado State University, Technical Report CS-93-103, 1993.
- [8] J. H. Holland, *Adaptation in Natural and Artificial Systems*. Ann Arbor: University of Michigan Press, 1975.
- [9] D. Kozinska, O. J. Tretiak, J. Nissanov, and C. Ozturk, "Multidimensional Alignment Using the Euclidean Distance Transform," *Graphical Models and Image Processing*, vol. 59, pp. 373-387, 1997.
- [10] W. M. Wells, P. Viola, H. Atsumi, S. Nakajima, and R. Kikinis, "Multi-Modal Volume Registration by Maximization of Mutual Information," *Medical Image Analysis*, vol. 1, pp. 35-51, 1996.
- [11] J. Nissanov, J. Eilbert, O. J. Tretiak, S. Gefen, S. Schremmer, C. Gustafson, and L. Bertrand, "3D Atlases - Bridges Between Neurogenomics and Neuroanatomy," presented at IEEE International Symposium on Bio-medical Imaging, Washington DC, 2002.
- [12] G. D. Rosen, A. G. Williams, J. A. Capra, M. T. Connolly, B. Cruz, L. Lu, D. C. Airey, K. Kulkarni, and R. W. Williams, "The Mouse Brain Library" presented at Int Mouse Genome Conference, 2000.
- [13] P. R. Woods, S. T. Grafton, C. J. Holms, S. R. Cherry, and M. J. C., "Automated Image Registration: I. General Methods and Intramodality Validation," *Journal of Computer Assisted Tomography*, vol. 22, pp. 139-152, 1998.
- [14] C. Gustafson, O. Tretiak, L. Bertrand, and J. Nissanov, "Design and Implementation of Software for Assembly and Browsing of 3D Brain Atlases," *Computer Methods and Programs in Biomedicine*, vol. 74, pp. 53-61, 2004.